Magnonic Crystal as a Medium with Tunable Disorder on a Periodical Lattice

J. Ding,[1] M. Kostylev,[2] and A. O. Adeyeye[1,*]

[1]*Information Storage Materials Laboratory, Department of Electrical and Computer Engineering, National University of Singapore, Singapore 117576*

[2]*School of Physics, University of Western Australia, Crawley, Western Australia 6009, Australia*

(Received 31 January 2011; published 21 July 2011)

We show that periodic magnetic nanostructures represent a perfect system for studying excitations on disordered periodical lattices because of the possibility of controlled variation of the degree of disorder by varying the applied magnetic field. Magnetic force microscopy images and ferromagnetic resonance (FMR) data collected inside minor hysteresis loops for a periodic array of Permalloy nanowires were used to demonstrate correlation between the type of FMR response and the degree of disorder of the magnetic ground state.

DOI: 10.1103/PhysRevLett.107.047205 PACS numbers: 75.78.−n, 75.30.Ds, 75.75.−c, 78.67.Pt

Arrays of magnetic nanowires (MNW) have generated considerable scientific interest due to their potential application for microwave devices [1,2] and domain wall logic [3]. On the other hand they represent a variety of artificial crystals [4] in which wave excitations can propagate. Magnetic artificial crystals are called magnonic crystals (MC), the wave excitations of which are collective spin wave (magnonic) modes which exist in the microwave frequency range [5–9]. In contrast to photonic [4] and sonic [10] crystals magnonic crystals are easily frequency tunable by applying magnetic field to the structure. MC response at remanence currently attracts a lot of attention ([9,11–13]). Minimizing the bias magnetic field applied to a nanostructure is important for possible applications in tunable microwave devices.

Magnetic periodic nanostructures may have a number of periodic magnetic configurations (magnetic ground states) for the same periodic geometry of the material, and the material can be switched between these ground states. Controlling of the magnonic frequency gap by switching between two ground states [9] and reconfiguration of a magnonic crystals has been recently demonstrated ([11,12]). Importantly, in these previous experimental studies additional microwave responses were seen within the hysteresis loops which are not present in the theories which assume a perfect magnetic periodic order for the array [9,11]. It was supposed that these branches originate from *magnetic* disorder on the periodic lattice. In the present paper, we experimentally show that these branches indeed originate from deviation from a perfect magnetic periodic order. This deviation takes the form of ''magnetic defects'' which represent individual wires (''single-site defects'') or *small* clusters of wires (''extended defects'') in which magnetization vector points in the opposite direction with respect to the average magnetic order of MC [14].

Defects on a crystal lattice are objects of fundamental importance: this can result in weak localization of electron on a crystal lattice in a condensed matter [15]; Anderson localization can occur due to disorder in various systems, such as condensed matter [16], Bose-Einstein Condensate [17], and photonic crystals [18,19] (see also extensive literature in all those papers). To study the effects of disorder and defects on a crystal lattice is not simple. Often one has to fabricate a large number of samples with different degrees of disorder, but otherwise identical, like it was recently done in Ref. [15]. In this Letter, we study the effect of magnetic disorder on magnonic excitations on the lattice of a 1D MC in the form of an array dipole coupled MNWs [6]. We demonstrate that this material represents an excellent model system for studying disorder because of the possibility of controlled variation of disorder degree by varying a magnetic field applied to the sample.

Twenty identical arrays of densely packed $Ni_{80}Fe_{20}$ MNWs were fabricated directly on top of a coplanar waveguide (CPW) using electron beam lithography, E-beam evaporation and lift off processing. Figures 1(a) and 1(b) show the SEM images of the CPW and two periods of alternating width MNWs. The arrays are spaced 5 μm from each other [see inset to Fig. 1(a)] to decouple them magnetostatically. The X, Y, and Z (out-of-plane) axes of a Cartesian frame of reference are parallel to the length $l = 10$ μm, width w and thickness $t = 30$ nm of MNWs, respectively. Each period consists of two MNWs with different widths $w_1 = 260$ nm and $w_2 = 220$ nm ($\Delta w = w_1 - w_2$). The edge-to-edge spacing g is 60 nm. Thus, the structure period is $w_a = w_1 + w_2 + 2g = 600$ nm. The array size in the direction of the array periodicity is 19.8 μm.

The magnetic ground state of MNW arrays was characterized using a magneto-optical Kerr effect magnetometer (MOKE) with a laser spot size of about 10 μm and by magnetic force microscopy (MFM). We also measured the unpatterned 30 nm $Ni_{80}Fe_{20}$ reference film using a vibrating sample magnetometer. We found a value for saturation

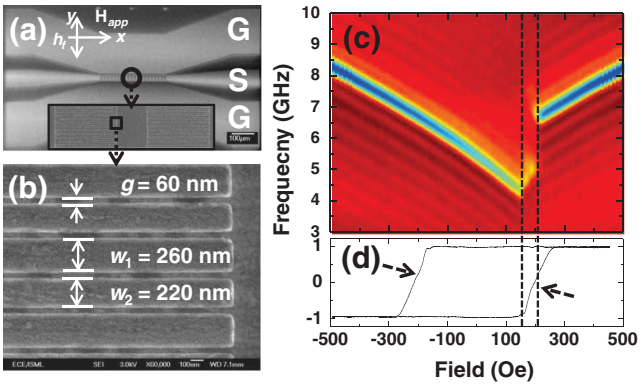

FIG. 1 (color online). (a): SEM image of the CPW line and of two nanowires arrays (inset). (b): SEM image of the alternating width nanowire array ($w_1 = 260$ nm, $w_2 = 220$ nm and edge-to-edge separation $g = 60$ nm). (c): Full loop 2D FMR absorption spectra for the array. (d): Normalized M-H loop for the array.

magnetization of 850 emu/cm^3, coercivity of about 2 Oe and a uniaxial anisotropy field of 4 Oe. The latter two values are negligible when compared with the coercivity of the isolated MNWs with $w = 220$ nm and 260 nm measured using MOKE.

The MFM study of the arrays showed that their magnetic behaviors were statistically identical. Therefore below we do not distinguish between MOKE and FMR responses of the total system of 20 arrays and the respective responses of individual arrays.

The FMR response was measured in the 1–20 GHz range using a microwave vector network analyzer (VNA). To obtain a high frequency response, VNA is connected to CPW by a ground-signal-ground microwave probe [9]. The magnetic radio frequency field h_f of CPW is applied along the Y direction, while an external static magnetic field ($H_{\rm app}$) is along the X direction as shown in Fig. 1(a). FMR measurements were performed by sweeping the frequency for fixed $H_{\rm app}$. This was repeated for a number of minor hysteresis loops for the sample. Each time we started from the negative saturation field $-H_{\rm sat} = -500$ Oe, passed through zero, and then gradually increased the field to a maximum $H_{\rm max} < H_{\rm sat}$ (forward half of a loop). The field is then subsequently decreased to $-H_{\rm sat}$ (backward half of a loop). A number of minor loops with different values of $H_{\rm max}$ were run. At the end of each loop, an MFM image of the remanent state was also taken after the $H_{\rm app}$ had been increased again from $-H_{\rm sat}$ to the same $H_{\rm max}$ and then switched off.

Figure 1(c) displays the absorption spectra for the forward half of the major hysteresis loop for the sample ($H_{\rm app}$ ranges from -500 Oe to $+500$ Oe). A stepwise increase in the resonance frequency is seen between 140 and 210 Oe and can be attributed to the reversal of magnetization in the wider wires [11]. A magnetic ground state which is characterized by alignment of the static magnetization vector with $H_{\rm app}$ for the wider wires and the counteralignment of them for the narrower wires [''antiferromagnetic'' (AFM) ground state] is expected for this field range for $g = 60$ nm, as the theories in [20,21] predict. The normalized MOKE data shown in Fig. 1(d) are in agreement with this type of the ground state. From this panel, one sees that the slope of the hysteresis loop slightly changes around $H_{\rm app} = 170$ Oe (indicated by the dashed arrows) which evidences transition to the AFM state. Importantly, we do not see formation of a plateau, which was observed in the hysteresis loops in Ref. [22] (Figs. 3 and 4 in that paper). This suggests that the AFM state is not stabilized on the *major* hysteresis loop for a range of applied fields in the present case of small values for Δw and g. Rather, in agreement with a small squareness of the hysteresis loop in Fig. 1(d), a gradual transition from a ferromagnetic (FM) ground state through an AFM one to a new FM state is expected. However, the AFM and the other ground states are easily stabilized on *minor* hysteresis loops. This was the main reason why we chose a value of Δw this small: it allows formation and repeatable stabilization of the largest variety of magnetic ground states in a large $H_{\rm app}$ range.

We took minor loop FMR absorption spectra in the $H_{\rm app}$ range from -500 Oe to $H_{\rm max}$. Figures 2(a-1) to (a-6) demonstrate these spectra for the relevant range -200 Oe to $H_{\rm max}$ (with 128 Oe $\leq H_{\rm max} \leq$ 220 Oe for different loops). For clarity, only the backward half of the loop, for which $H_{\rm app}$ decreases from $H_{\rm max}$ to $-H_{\rm sat}$, is shown. The forward halves of the loops are trivial: each of them coincides with the section $H_{\rm app} \leq H_{\rm max}$ of the spectrum in Fig. 1(c) for the respective value of $H_{\rm max}$.

Panels b-1 to b-6 of Fig. 2 display the corresponding MFM images taken at remanence. The wires are oriented horizontally. Two vertical lines close to the image edges consisting of either brighter of darker spots than the rest of the area (''edge contrast lines'') are signatures of the wire edges. A bright spot is consistent with the static magnetization vector pointing away from the wire edge and the dark spot is for the tip of magnetization vector pointing to the respective wire edge. First one observes that for each bright or dark spot at one edge of the array there is a respective spot of the opposite contrast (dark or bright) at the opposite edge. This fact together with an absence of signatures of stray fields of domain walls inside the array evidences that all the wires are in a homogeneous (single-domain) magnetization state in all panels. This is in agreement with the very small in-plane aspect ratio for the wires (0.022 and 0.026, respectively).

The degree of magnetic disorder varies between the panels. We quantify the disorder degree by performing a Fourier transform of the distribution of the MFM contrast along one of the edge contrast lines. The insets to panels b-1 to b-6 display the Fourier spectra along with the ratio of the amplitudes r_1/r_0 of two important Fourier harmonics. One (r_1) corresponds to the Fourier wave number k_1 equal

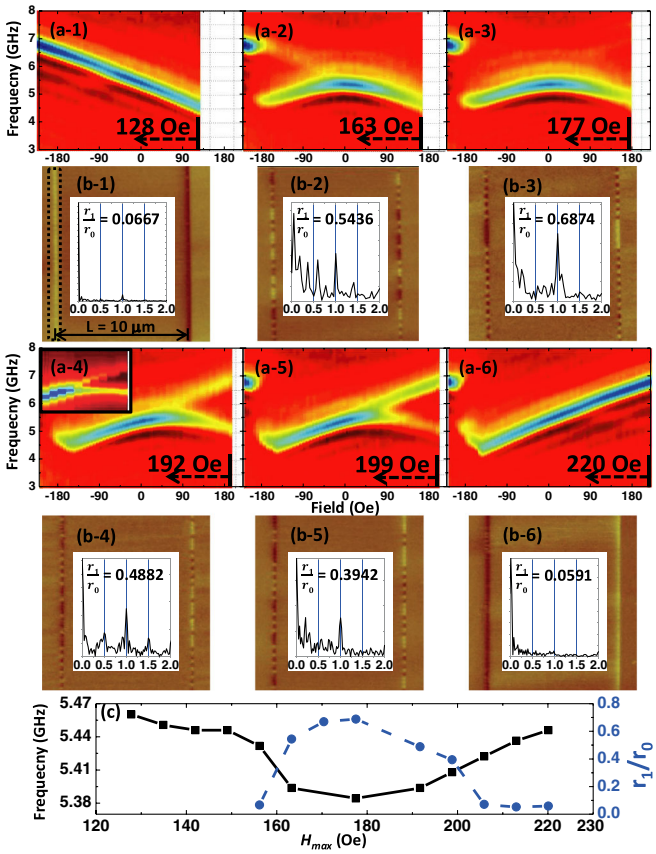

FIG. 2 (color online). (a-1) to (a-6): FMR absorption spectra inside the minor loops with $H_{\max} = 128$ Oe, 163 Oe, 177 Oe, 192 Oe, 199 Oe and 220 Oe. Inset to (a-4): example of 1D simulation. (b-1) to (b-6): MFM images for the same $H_{\max}$ at remanence. Insets: Fourier transforms of the respective MFM data. (c) Frequency of the fundamental mode at remanence (solid line) and the ratio r_0/r_1 (dashed line) as a function of $H_{\max}$.

to the lattice vector $G = 2\pi/(w_1 + w_2 + 2g)$, and the other ($r_0$) to the zero wave number $k = 0$. One sees that the richest spectrum displaying a largest number of harmonics for $k/G < 1$ is in the inset to Panel b-2. Indeed, the edge contrast for this state is the most irregular. Additional harmonics but of smaller relative amplitudes than in panel b-2 are also seen in Panels b-4 and b-5. They correspond to $k = G/2$, $k = G/3$, and $G/4$. By comparing these data with the respective MFM images one finds that the ground states are more regular in these cases. Panel b-3 displays just two prominent peaks for $k = 0$ and for $k = G$ and is characterized by the maximum value of r_1/r_0 [see Fig. 2(c)]. The Fourier peak at $k/G = 1$ corresponds to the AFM order. Indeed, the respective MFM image displays an almost perfect AFM order.

Panel 2(a-1) is characterized by a single monotonically falling branch ($\omega(H_{\text{app}})$). The respective MFM image shows that this response originates from a ground state with a perfect FM order with the static magnetization vector pointing to the right [Fig. 2(b-1)]. Similarly, the growing branch in Fig. 2(a-6) existing for of $\omega(H_{\text{app}})$ for $H_{\text{app}} - 120$ Oe is identified as a FMR response of the perfectly ferromagnetic ground state with the static magnetization vector pointing to the left [Fig. 2(b-6)]. This identification is in agreement with the theory of collective modes for the FM state [9,11].

The (H_{app}) curve in Fig. 2(a-3) is nonmonotonic. In Ref. [9] this branch has been identified as the fundamental acoustic collective mode for the antiferromagnetic state. From Fig. 2(b-3) one sees that, indeed, the ground state for this minor hysteresis loop is AFM. This represents an experimental evidence for the previous identification [9] which was based solely on the theory. The experimentally observed state is actually not perfectly AFM, a 3-period long extended FM defect is observed in the middle of the MFM image. This suggests that a faint response existing for $H_{\text{app}} > 0$ and monotonically growing in frequency with H_{app} is one of the defect.

Let us now discuss the responses for the states which are transitional between the well ordered FM and the AFM states [Figs. 2(a-2), 2(a-4) and 2(a-5)]. The main observations which can be drawn from these panels are as follows. (i) The FMR response for the transitional states looks like combination of the responses for the FM and the AFM states in Figs. 2(a-1), 2(a-6) and 2(a-3), such that the respective branches can be termed "FM" and "AFM" branches. (ii) Linewidths for the observed resonance peaks do not vary noticeably with H_{app} across each minor loop and between the loops and are very close to the linewidth obtained on a reference continuous film (the full linewidth is 0.5 GHz). (iii) The shape of the AFM branch and the mode frequency at remanence varies between the loops [Fig. 2(c)] and is correlated to r_1/r_0.

In order to explain these features numerical simulations based on a 1D version of the model from [23] have been performed. The ground states for the linear dynamics simulations were assumed to be the same as observed in the respective MFM images [Figs. 2(b-1) to (b-6)]. To this end the experimental contrast line data were digitized such that $+1$ corresponds to static magnetization vector pointing to the right and -1 to one pointing to the left [Fig. 3(a)–3(c)]. Periodic boundary conditions (PBC) at the right- and left-hand edges of Figs. 3(a)–3(c) were assumed. We used the values for the saturation magnetization and for the resonance linewidths extracted from the FMR data obtained on the reference sample.

An example of the results of simulation of a frequency vs applied field dependencies is shown as an inset to Fig. 2(a-4). One sees a good qualitative agreement with the experiment. The simulated mode profiles for the disordered state are complicated (Fig. 3). The simplest ones are observed for the ground state of Fig. 2(b-3). The AFM ground state in Fig. 3(b) contains an extended FM defect. Accordingly, one observes one extended dynamic state of AFM nature [Fig. 3(e)] outside the defect whose amplitude noticeably decreases on the defect. This mode is

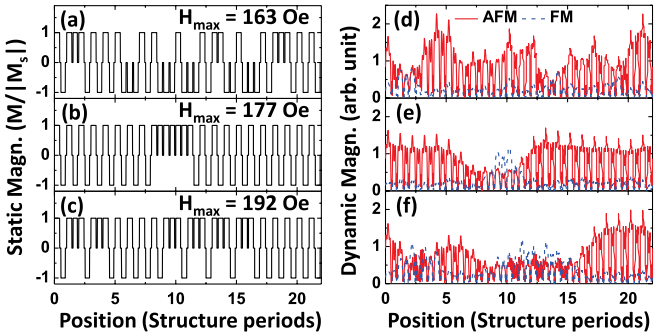

FIG. 3 (color online). (a)–(c): The magnetic ground states for $H_{max} = 163$ Oe, 177 Oe and 192 Oe, respectively. (d)–(f): the respective calculated profiles of dynamic magnetization. Red solid line: AFM mode; blue dashed line: FM mode. A 1D numerical model has been used in this calculation.

responsible for the main peak of the FMR response. The defect has its own mode. Localization of the defect mode on the defect is relatively strong: the amplitude of the mode half a way between two neighboring defects (recall PBC) is about 20% of the maximum inside the defect. For this reason the FMR response of this mode is weak, and is consistent with a faint FM-type response seen in Fig. 2(a-3). It is appropriate to term this weak response as an ''impurity'' or ''defect'' dynamic state of MC.

The ground state in Fig. 3(a) [corresponds to Fig. 2(b-2)] can be characterized as an AFM one with multiple *single-site* FM defects. A single-site FM defect inside an AFM environment results in a FM cluster 3 wires long. From Fig. 3(d), one sees that the dominating mode is the lower-frequency AFM mode. The higher-frequency FM mode has considerably smaller excitation amplitude which is in full agreement with Fig. 2(a-2). Both modes are more extended than in Fig. 3(e) and the picture shows less regularity, but still localization of particular modes on particular clusters, FM or AFM ones, is clearly seen. Again, one can characterize the FM mode as a defect or impurity state based on the above considerations.

The ground state in Fig. 3(c) [corresponds to Fig. 2(b-4)] can be regarded as two defectless AFM clusters (4th–9th periods and from 16th period onwards) and two FM clusters (2–4) and (9–15) each having a number of single-site AFM defects (1 and 3 defects, respectively). As in Fig. 3(d) one observes that a small number of single-site defects does not prohibit formation of a fundamental collective mode of a cluster, in this case of one of the FM type. Both AFM and single-site-defect containing FM dynamic states again have a noticeable amplitude on the clusters of the different type. The excitation amplitudes of these two modes are comparable which is in agreement with the experimental data in Fig. 2(a-4). This case clearly demonstrates potential of the wire arrays as a model medium for studying effects of disorder: a simple magnetization procedure transforms a state of AFM type with FM impurities [Fig. 3(d)] into a state of FM type with AFM impurities.

Similar to the experiment [Fig. 2(c)], our simulation has also shown that mode frequencies for the transitional states deviate from ones for the respective frequencies for the arrays in the perfect FM and AFM states. This is an evidence of strong interaction of the defects with their environment.

In conclusion, we studied magnetic disorder on the arrays of dipole coupled nanowires. We found experimental evidence that switching of nanowires produces a disordered magnetic ground state inside the hysteresis loop. Collective dynamic states localized on clusters of nanowires with different magnetic orders are formed and the respective FMR response inside the hysteresis loop represents a doublet, whereas outside the loop the fundamental oscillation is a FM singlet. Depending on the magnetization history either AFM or FM state of the doublet can be either a fundamental or a defect (impurity) one. Localization of these dynamic states on the respective wire clusters is not very strong, the states extend into the clusters of different magnetic order such that their amplitude is noticeable everywhere. Single-site magnetic defects do not prohibit formation of collective modes.

We acknowledge financial support from the National Research Foundation, Singapore under Grant No. NRF-G-CRP 2007-05, SMF-NUS New Horizon Awards, and from the Australian Research Council.

*Corresponding author.
eleaao@nus.edu.sg

[1] S. Choi *et al.*, Phys. Rev. Lett. **98**, 087205 (2007).
[2] H. Zhang *et al.*, Appl. Phys. Lett. **95**, 232503 (2009).
[3] X. Zhu *et al.*, Appl. Phys. Lett. **87**, 062503 (2005).
[4] E. Yablonovich *et al.*, J. Opt. Soc. Am. B **10**, 283 (1993).
[5] S. A. Nikitov *et al.*, J. Magn. Magn. Mater. **236**, 320 (2001).
[6] G. Gubbiotti *et al.*, J. Phys. D **43**, 264003 (2010).
[7] S. Neusser *et al.*, Adv. Mater. **21**, 2927 (2009).
[8] V. V. Kruglyak *et al.*, Phys. Rev. Lett. **104**, 027201 (2010).
[9] J. Topp *et al.*, Phys. Rev. Lett. **104**, 207205 (2010).
[10] T. Miyashita, Meas. Sci. Technol. **16**, R47 (2005).
[11] S. Tacchi *et al.*, Phys. Rev. B **82**, 184408 (2010).
[12] R. Zivieri *et al.*, Phys. Rev. B **83**, 054431 (2011).
[13] A. Barman *et al.*, J. Phys. D **43**, 422001 (2010).
[14] We call a sequence of wires in the same magnetic ground state a cluster to avoid confusion between the clusters and usual domains inside individual magnetic elements.
[15] Y. Niimi *et al.*, Phys. Rev. Lett. **102**, 226801 (2009).
[16] P. W. Anderson, Phys. Rev. **109**, 1492 (1958).
[17] J. Billy *et al.*, Nature (London) **453**, 891 (2008).
[18] S. John, Phys. Rev. Lett. **58**, 2486 (1987).
[19] Y. Lahini *et al.*, Phys. Rev. Lett. **100**, 013906 (2008).
[20] E. Y. Tsymbal, Appl. Phys. Lett. **77**, 2740 (2000).
[21] R. Alvarez-Sanchez *et al.*, J. Magn. Magn. Mater. **307**, 171 (2006).
[22] S. Goolaup *et al.*, Phys. Rev. B **75**, 144430 (2007).
[23] S. Tacchi *et al.*, Phys. Rev. B **82**, 024401 (2010).